Collisions of ^{238}U with Pb and Be targets at 750 A.MeV investigated at the FRS

M. Bernas

IPNO DRE 97-22

COLLISION OF ^{238}U WITH Pb AND Be TARGETS AT 750 A.MeV INVESTIGATED AT THE FRS.

M. Bernas, for the FRS collaboration (GSI-Darmstadt), IPN-Orsay, CRN-Strasbourg (IN2P3), Warsaw-Univ. and TH-Darmstadt

Conference nucleus-nucleus 97
Gatlinburg 2-6 Juin 1997

Collisions of ^{238}U with Pb and Be targets at 750 A.MeV investigated at the FRS

M. Bernas, for the FRS collaboration (GSI-Darmstadt), IPN-Orsay, CRN-Strasbourg (IN2P3), Warsaw-Univ. and TH-Darmstadt

Abstract

Projectile fission of ^{238}U was investigated at a bombarding energy of 750 A·MeV using Pb and Be targets. The fully stripped forward emitted fragments from Ca up to Nd were analyzed with the Fragment Separator (FRS) and unambiguously identified by their energy-loss and time-of-flight. From kinematics and from comprehensive isotopic distributions, the low energy fission, high energy fission and fragmentation regimes could be investigated.

1 Introduction

A main goal of nuclear physics is to understand the behaviour of nuclear matter at finite and ultimately at high temperatures. Eventhough the nuclear fission has been studied for many decennies and is known to occur only after dissipation of excitation energy, it remains one of the most fascinating process of collective flow of nuclear matter and the ideal example for the many body problem. Fission of excited nuclei is difficult to investigate. After being strongly excited the energy is dissipated via particles, nucleons and γ emission and somewhere along the path, a fission may occur. The difficulty comes from ignoring which isotopes undergo fission at which excitation energies. Extensive studies have been performed after fusion reactions [1] in order to scale the times involved at each stage of the energy release. In fusion collective effects are playing an important contribution. Other experiments were performed on ^{238}U fission after collisions induced by p at various incident energies [2] [3] [4], by light heavy ions [5] [6] [7], and by $\overline{p}$ [8]. We report here on the isotopic yield distributions of fission fragments produced after nuclear collisions of a ^{238}U beam with Pb and Be target nuclei. Despite improvements of the target handling, spectrometers, and detection systems, the direct separation and investigation of fission fragments by recoil-in-flight separation remains difficult due to the broad ionic charge state distribution of fission products. The direct separation is even impossible for the heavy group of fission fragments due to limitations of the Z resolving power at low energies. Furthermore, studies of extremely low production yields are difficult to perform, since recoil spectrometers have rather small solid angles, while the fragments are emitted isotropically. These new data provide a complementary insight on the regime of fission of excited U-fragments, on the nature and on the excitation energy of the intermediate system.

2 Experiment

Acceleration of a ^{238}U beam to relativistic energies by using the heavy ion synchrotron SIS at GSI provides a new vista of the fission process. The use of inverse kinematics at high energies to induce fission in peripheral collisions has three main advantages:

1) The momenta of the fragments are focussed into a small cone centered around the beam direction and their velocities are almost constant. Thus, fragments are efficiently transmitted through a separator.

2) The fragments are totally stripped of electrons, i.e. their charge state equals their atomic number and ambiguities when dealing with different charge states can be totally avoided.

3) At these high velocities, fragments can be identified by Bρ-ΔE-ToF techniques. Two experiments have been performed with a ^{238}U beam at the energy of 750 A·MeV. In the first measurement a beam of 2· 10^5 U ions/s, was impinging on targets of Be and Pb of 1 g/cm^2 and 1.25 g/cm^2 thickness. The high Z target was chosen to favour fission following electromagnetic processes. Reaction products were analyzed with the fragment separator FRS [9] which was operated in the achromatic mode. Energy loss of the separated fragments, which is characteristic for their nuclear charge Z, was measured in a four-stage MUSIC ionization chamber at the exit of the FRS. For each fragment, the deflection radius ρ in the last two dipoles was determined from the position of the trajectory in the intermediate and in the final focal planes measured with two plastic scintillator counters. The velocity β was measured from the time of flight between these two scintillators over 37 m. Thus knowing Bρ, Z and the velocity, the mass A was calculated event-by-event. For fragments of similar velocities, the magnetic deflection separates isotopes according to the mass-to-charge ratio, A/Z. A survey of production rates in terms of A/Z was obtained with successive tunings of the magnetic fields over the appropriate rigidity range (32%).

The fission kinematics at relativistic energy has been described [10] [11] as follows: The momentum of the emitted fragment results from the Lorentz composition of projectile and fission momenta. The corresponding vector lies in a cone, and it ends on an ellipsoidal shell. The thickness of the shell is given by the variance of the velocity distribution of the fission fragments. This momentum phase space is truncated by the angular and momentum acceptances of the FRS as pictured on Fig. 1.

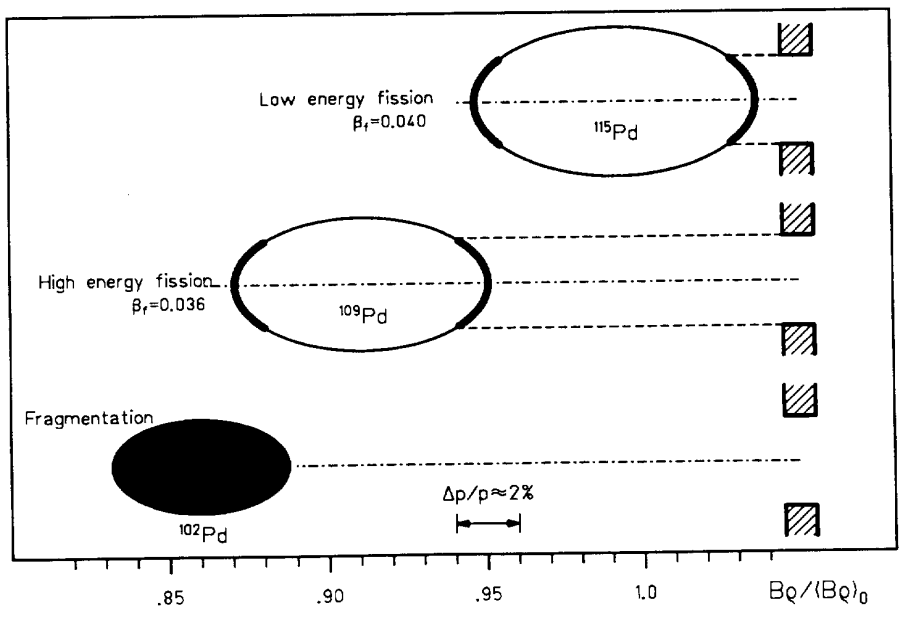

Fig. 1 : Momentum phase space of fission fragments from relativistic ^{238}U projectiles colliding with Pb target nuclei.
a) L.E.F; The angular and momentum acceptances of the FRS select forward or backward emitted fragments separated by $\Delta p/p$ = 9 % for Pd.
b) H.E.F; Fission of excited fragments leads to less n-rich isotopes and thus the momenta of fragments are reduced.
c) For fragmentation the volume of the small ellipse due to statistical momentum transfer is filled.

For low energy fission the velocities of forward (or backward)-emitted fragments are higher (or lower) by about 5% as compared to the projectile velocity. They are selected within the angular (15 mr) and momentum (2%) aperture of the FRS, as shown on Fig. 1a. Neutron rich isotopes with A/Z larger than in ^{238}U can be produced when only few neutrons are evaporated by the most peripheral collisions. Therefore, low energy fission is selectively observed at the largest longitudinal momenta (Fig. 1a). At lower magnetic rigidities, decreasing A/Z fragments are selected by the FRS. On Fig. 1b we have illustrated the selection of forward high energy fission (HEF) fragments characterized by a lower A/Z ratio and similar velocities as fragments from low energy fission (LEF). They come in the same momentum window as the backward emitted fission fragments from a low excitation energy. At even lower rigidities products from U-fragmentation are selected by the FRS together with backward fragments from LEF (Fig. 1c). The momentum space filled by projectile fragmentation products is represented. The velocity of those products is close to the projectile velocity, but their masses are much lower due to the many neutrons evaporated. Thus the corresponding rigidities are well below the beam rigidity.

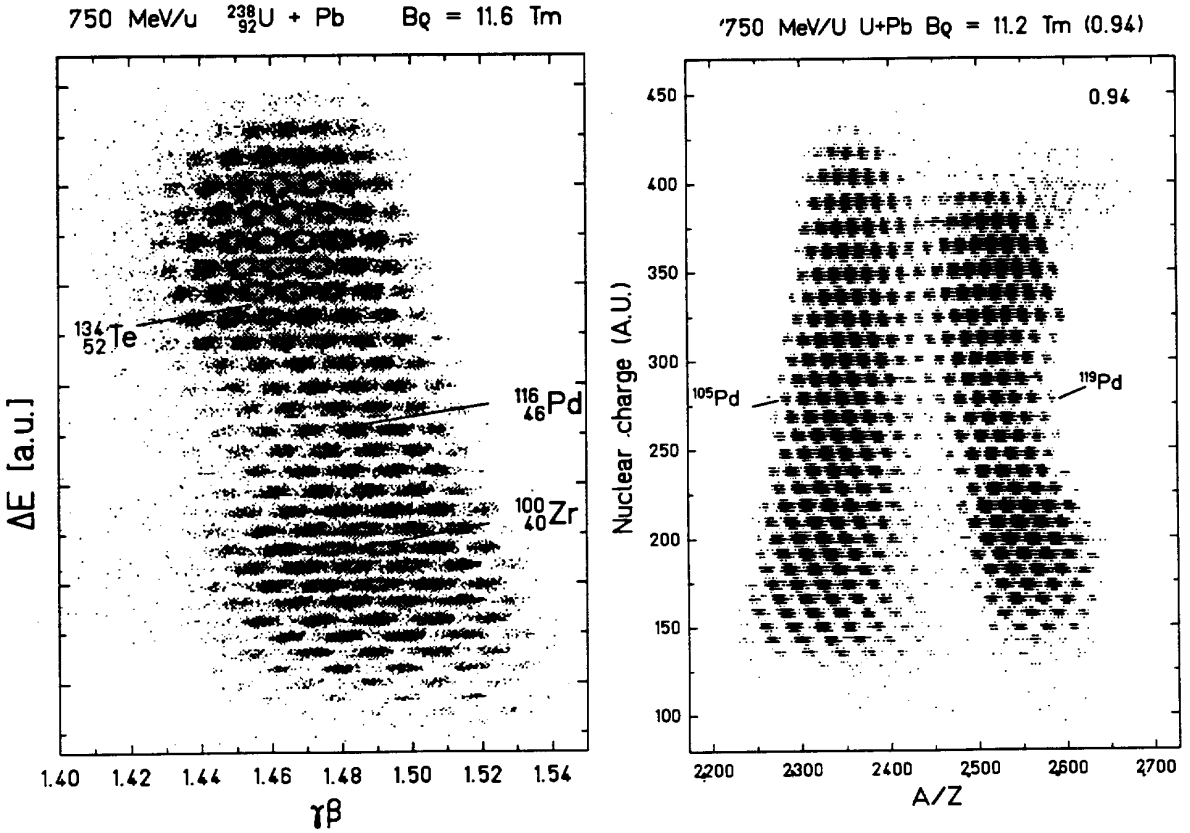

Fig. 2 and 3: Scatter-plots ΔE versus A/Z of the isotopes transmitted by the FRS at rigidity 4% above 6% below the projectile rigidity.

The FRS was tuned on the light group of fission fragments (Z=40), the heavy fragments ($Z > 50$) as well as the very light ones ($Z < 30$) were cut and beyond Z=58 no fission fragments were detected. The angular aperture of the FRS and the energy broadening due to the target thickness reduce the transmission through the FRS: Values of 2.8% for Sr-fragments and 5% for Te-fragments were calculated by using the Monte-Carlo simulation code MOCADI [12] where fission kinematics has been included.

3 Low energy fission Results

The scatter-plot of isotopes separated with the FRS from the fission of U on a Pb target at a magnetic rigidity of 4% above that of the projectile, $(B\rho)_o$, is shown in fig. 2.

Because of the rather thick Pb target, the selected fragments cover a range of velocities $\Delta\beta\gamma$ / $\beta\gamma \approx 4\%$ due to target location straggling effects, and hence a number of ≈ 4 masses/element are transmitted simultaneously [10].

The double-humped Z distribution well-known from low energy fission clearly shows. The pair of partners ^{134}Te and ^{100}Zr is enhanced and the nuclei in the fission valley are seen with yields relatively higher than in thermal neutron induced fission [13]. Series of data taken at rigidities higher than projectile rigidities were integrated and corrected for transmission through the FRS. Peak/valley ratio and odd-even effect commonly used to scale the excitation energies of the fissioning nucleus lead to diverging values of 12 MeV and 20 MeV, respectively. This discrepancy was partly resolved by using the comparison with the data obtained on the Be target which reflect the contribution of nuclear fission [11]. It was concluded that the double dipole excitation of the U-projectile and nuclear interaction contribute to populate the symmetric mode. The ultimate analysis of the LEF regime was accomplished recently in the work of Donzaud et al. [14]. Between Z=40 and 52 the symmetric mode was separated from the tails of asymmetric fission. The contribution of this mode increases until Z=46 where it is responsible for 100% of the measured yields. Note that this mode helps to produce very neutron rich species in the region of niobium to palladium.

The largest Bρ setting for which fragments were still detected with sufficient intensity in the first experiment was limited by the rather low ^{238}U beam intensity and amounted to 1.08*$(B\rho)_0$. On the corresponding ΔE-ToF scatter-plot more than 50 new neutron rich isotopes were discovered within 10 hours of data taking [10]. The most abundant one observed was the doubly magic ^{132}Sn produced then at a rate of about 1 event/s. The cross sections for fission of low excited ^{238}U were measured independantly and found to be 0.12 and 2.1 barn (within an accuracy of 15%) on Be and Pb, respectively [16]. The lower limit of measurable cross-sections was about 1 μb.

In the second experiment a Be target was chosen to widen the range of elements produced by fission. With a beam a hundred times more intense and a counting time of 130 h the limiting cross-section was decreased down to 0.3 nb and at $B\rho = 1.16^*(B\rho)_0$, a second wave of 57 new n-rich nuclei were identified including the doubly-magic isotope of ^{78}Ni [15]. The ratio A/Z reaches 2.8 between Ca and Zr [17].

In the region of symmetric fission, where yields are much higher than in low energy fission, six isotopes were discovered for Nb, Mo ,Ru, Rh, and Pd in the two experiments. Note that previous studies in this region were performed with the IGISOL facility by

using 20 MeV proton-induced fission of ^{238}U [18]. The new nuclear species observed in our measurement fill the gap of elements not accessible by chemistry or by ISOL ion source techniques.

Our experiment reveals not only a new landscape of fragments, hidden until present, but represents also the first ΔE-ToF isotopic identification of heavy fission fragments. Such a direct separation leads to accurate relative fission yields, free from any chemical bias. Moreover, the 300 ns required for the ions to pass through the FRS are shorter than any β decay halflives so the measured yields cannot be influenced by fast β^--decays.

4 High energy fission

At smaller impact parameters in case of nuclear collisions one or few nucleons are abraded from the U-projectile. The residual "prefragment" is left excited. Excitation energy is released by the emission of nucleons(mainly neutrons) or nucleides. Along the deexcitation process a residue can undergo fission. Therefore the fragments are less neutron rich than in low excitation fission. The total kinetic energy of fission (TKE) stays almost the same. The fragment momenta are lower and, on Fig. 1, the ellipse becomes slightly shrinked and shifted down because of the neutron losses.

On Fig. 3 the scatter plot obtained for $B\rho = 0.94^*(B\rho_0)$ illustrates the selection of low energy (LE) fission fragments emitted backward (A/Z= 2.55) together with other fission products with A/Z = 2.35 forward emitted. These last products reappear, for the backward emission, at a rigidity of $0.86^*(B\rho)_0$. They do not show the Z-asymmetric behaviour. They come from symmetric fissions of excited fragments with atomic numbers lower than 91. The production yield reaches its maximum in the region of Pd as expected for symmetric fission.

At the lowest magnetic rigidities investigated -0.86 and $0.82^*(B\rho)_0$- projectile fragments are clearly observed at A/Z = 2.2 (see Fig. 3). Isotopes of ^{112}Te, ^{97}Pd and ^{84}Zr for example belong to the class of p-rich nuclei in the corridor of fragmentation residues [19].

The purpose of the data-analysis is to characterize events due to fission at high excitation energy and to obtain the production yields for each fragment. The distribution of yields should reveal at which mass region this fission does occur, which fraction of the excitation is dissipated before fission and which fragments undergo fission with how much excitation energies.

After normalizing the spectra for the beam intensities and dead times of each measurement, the data were gathered isotope by isotope for each element as function of $\beta\gamma$ (Fig. 4). One can see the two peaks due to the FRS phase space truncation of forward and backward fission. They are centered around the primary beam value of $\beta\gamma$ and separated in momenta by a difference, $\Delta\beta\gamma$ / $\beta\gamma$ equals $\approx$ 9%, as expected for a binary fission process[11]. The yields associated to the lightest isotopes follow a wide single Gaussian centered on the beam $\beta\gamma$-value as expected from direct ^{238}U fragmentation. U-fragments are transmitted through the FRS ten times better than fission products. The analysis of fragmentation in the Z region under scope is reported in a forthcoming paper [20].

1) Fission velocities.

The velocity distributions characterizing fission fragments (Fig. 4) were fitted assuming that the shape was the same for isotopes of a given element since the c. m. fission velocity and the widths reflecting target location effects are the same for all isotopes (to first order). Those fits provided a few parameters, the c. m. fission velocities and widths as a function of Z, and the normalizations for each isotope which, accounting for a transmission coefficient lead to the production cross section for each isotope.

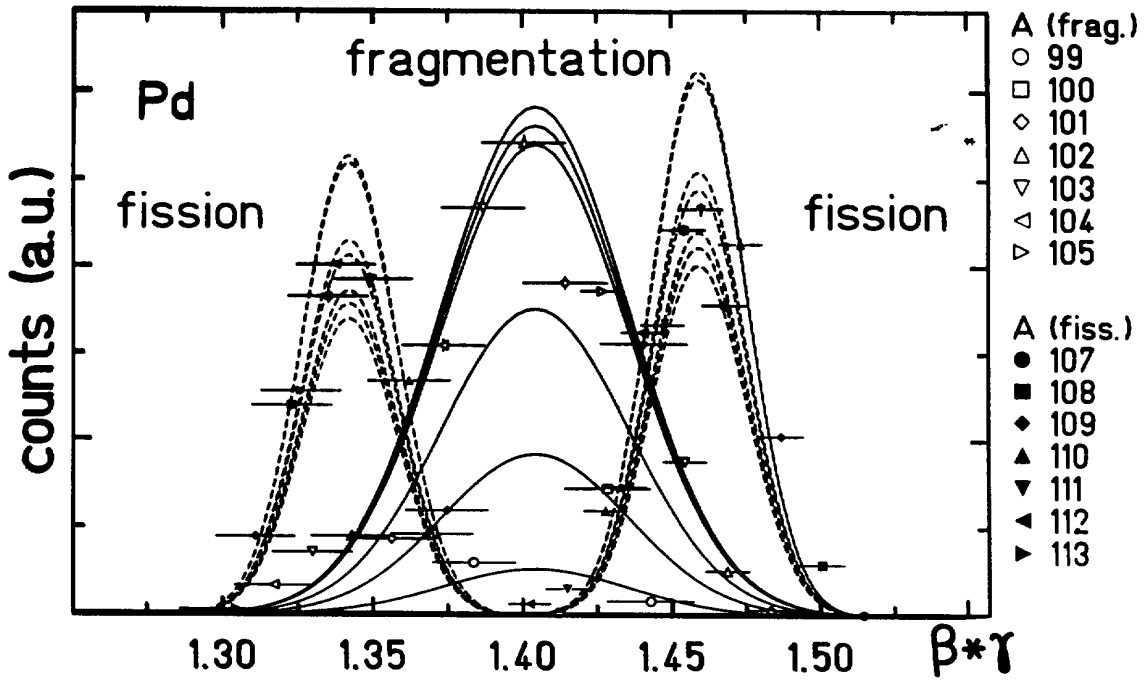

Fig. 4 : Velocity distribution of Pd isotopes measured over the four Bρ settings. The double humped structure is associated to transmission of forward and backward emitted fission products. The distribution of very neutron-deficient fragments is found to be centered around the beam velocity. Those fragments result from fragmentation. The width is larger due to the momentum transfer by the fragmentation process.

The c. m. velocities are slightly less than for LEF, mostly for very light Z fragments (Z<35) whereas the widths of the peak are found to increase. It can be qualitatively explained by the fact that light fission fragments are due to symmetric break-up of the U-fragments mainly produced (Z=88) superimposed with fragments of a similar break-up of lighter fragments (Z=80) for which the velocity, calculated according to Viola [21] is smaller.

2) Isotopic yields

Within our assumptions, the transmission is only a function of the atomic number Z and not of the mass A. It grows from 1.9% for Ge up to 4.8% for Sb isotopes. We took into account the small reduction in the c.m. fission velocity as compared to the low energy fission velocity, thus increasing slightly the transmission. Isotopic cross sections were calculated using these transmission values.

On Fig. 5 are shown comprehensive isotopic distributions of fission fragments for the elements investigated from Germanium up to Antimony. The neutron rich isotopes are produced by Coulomb (E.M.) and low energy nuclear (L.E.) fission. Next to this regime, less neutron-rich nuclei are observed with distributions centered at lower N/Z values, between 1.32 to 1.41. For light elements up to Mo and heavy elements Sn and Sb, the predominant peak due to E.M. and L.E. fission is rather well separated from a wider peak due to high energy (H.E.) fission. The total width of the isotopic distribution is increasing with the Z of the fragments. The contribution of the high energy (H.E.) fission increases with Z, and near symmetry it becomes the main process. In order to extract more precise information, Gaussians were fitted to the H.E. fission peaks of Fig. 5 assuming a symmetric shape for this component. In this way, the elemental cross sections, the variance and the mean neutron number for each element were determined.

3) Z and A distributions

The peaks associated to the H.E. fission process were integrated over the isotopes of each element and the elemental cross sections are plotted on Fig. 6.

- The element distribution (Fig. 6a) is centered around element Tc ($\overline{Z}$ = 42.9 $\pm$ 0.03) which shows that a mean number of 6 protons were released in the process. The FWHM of the distribution is found to be (16.2 $\pm$ 0.9) charge units. It is to be compared with the smaller values of 10.6 and 14.1 measured respectively for the E.M. [14] and nuclear symmetric fission modes in lighter fissionning nuclei recently investigated [25]. For the isotonic distributions, Fig. 6b a mean value of N = 58.1 $\pm$ 0.3 shows that during the different phases of the reaction, (30 $\pm$ 1) neutrons were taken from the fissioning nucleus. The mean A/Z values of the fragments are slightly increasing 2.32 to 2.42 with Z varying from 32 to 51. This compares to 2.59 for the projectile.

- The positions of the centroids $\overline{A}_{HF}$ extracted by the Gaussian fits are compared to the mean values $\overline{A}_S$ for stable nuclei, mean L.E. fission and fragmentation products on Fig. 7. For all elements $\overline{A}_{HF}$ is found larger than $\overline{A}_S$ by 3 units. However, at given neutron numbers the gaps between of the mean atomic number $\overline{Z}_{HF}$ and the corresponding value in the valley of stability $\overline{Z}_S$ increases with Z. There is a clear trend from a distance of about one unit for Ge to about 2.5 for Ag. This corresponds to a mean A/Z value of 2.32 and 2.27 for measured and stable Ge isotopes, respectively. For Ag these values are 2.39 and 2.30.

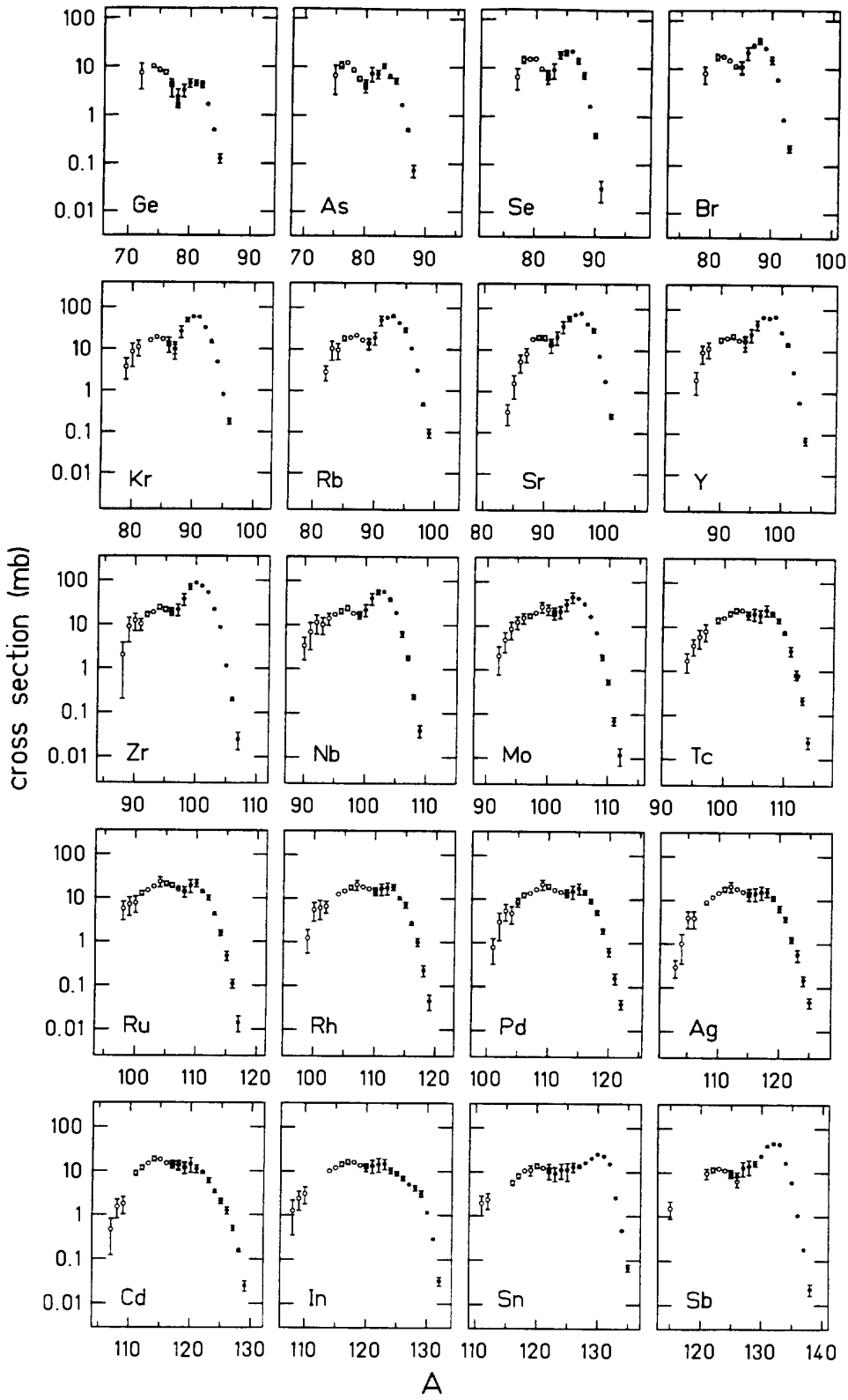

Fig. 5 : Production cross sections are given for the complete range of isotopes produced by fission. There is a gradual transition between the regimes of low energy and high energy fission. A clear separation is still possible.

- From both distributions, Fig. 6a and 6b, cross sections related to the H.E. fission regime were derived. We found (1.57 ± 0.11) b confirming the value of (1.4 ± 0.2) b obtained in an independant direct measurement [16].

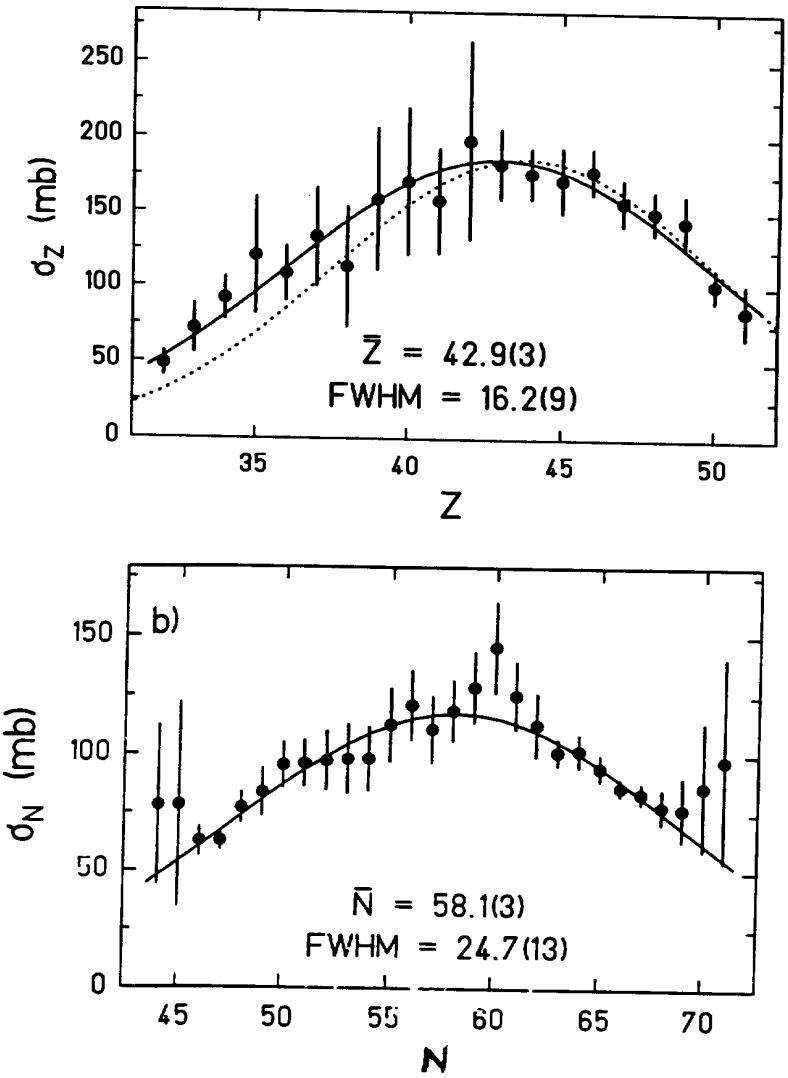

Fig. 6 : Elemental and isotonic cross sections $\sigma(Z)$ and $\sigma(A)$ obtained for the fission of excited fragments. The dashed line is the result of the simulation described latter in the text.

5 Discussion

From the isotopic yield distributions of fragments, the mean fissionning nucleus can be calculated using the knowlwedge on fragmentation, on nucleon emission during the cooling-off and the number of neutrons emitted at scission. Assuming a symmetric fission the parent nucleus would have an atomic number of 85.8 and a mass of 202. During the nuclear collision 6.2 protons and 19.8 neutrons were abraded or emitted from the ^{238}U nucleus. The final A/Z ratio around Z=42.9 is found very close to the value obtained in collisions of relativistic protons on ^{238}U [2]. However, in our experiment the abrasion-ablation by the Pb target is effective. The ratio of abraded protons π_{abr} to neutrons ν_{abr} should be proportional to the Z/N ratio in the primary nucleus, 92:146, with 27 MeV invested for each abraded nucleon [22]. The primary fragment cools off by evaporation of a few pro-

tons π_{evap} in the beginning of the evaporation cascade and of a large number of neutrons ν_{evap}. The average energy to evaporate a proton

$$e_p = S_{2p}/2 + B_f^{eff} + 2T$$

is estimated to be 21.9 MeV [23] with B^{eff} an effective Coulomb barrier, T the temperature and S the two nucleon binding energy. To free a neutron, the energy

$$e_n = S_{2n}/2 + 2T$$

is averaged over the evaporation cascade and assumed to be 9.9 MeV. When neutron evaporation times approach the time to overcome the fission saddle the competition with fission sets in. Each neutron emitted from a fission fragment carries away 8.9 MeV. In symmetric fission, at the barrier, three post-scission neutrons are freed which do not contribute to the energy balance. In total, a number of 7 post-scission neutrons is assumed and 42 MeV are released with the liberation of the 4 additional neutrons.

The energy transferred in the abrasion stage is liberated by the series of evaporation steps. The number of abraded particles ($\nu_{abr} = 6$ and $\pi_{abr} = 3.7$) and an energy transfer of (262 ± 17) MeV is determined from energy and particle conservation with the parameters given. The primary hot nucleus leading to our pair of fission fragments is ^{228}Ra. This nucleus evaporates a mean number of 16.8 neutrons and of 2.5 protons in an evaporation cascade carrying away 220 MeV and ending at ^{209}Rn. This nucleus fissions, emits the above 7 fission neutrons and ends up in a pair of ^{101}Tc.

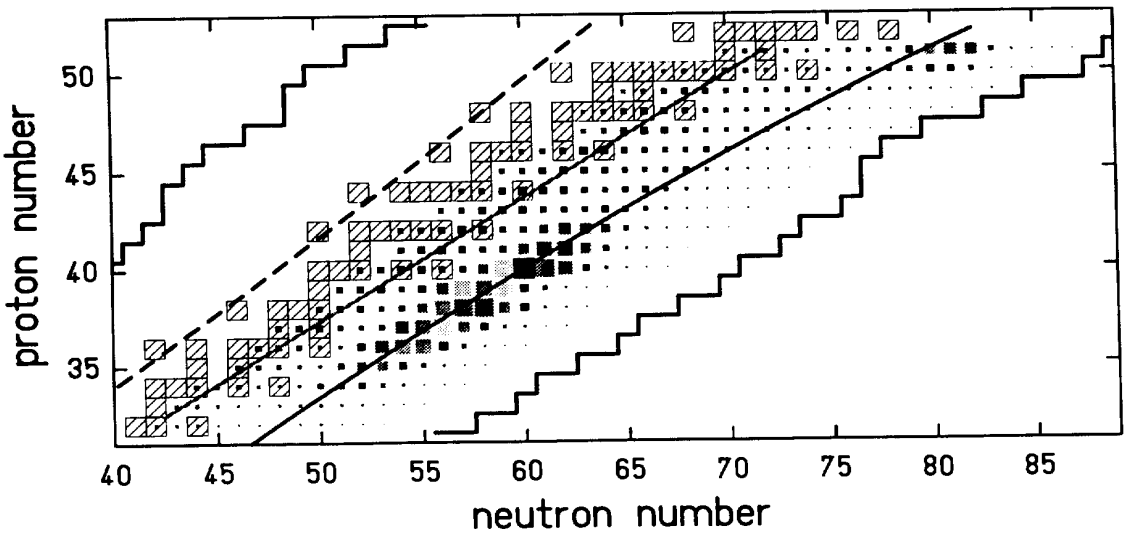

Fig. 7 : Nuclear chart showing with full lines the ridges of each fission regime. The dashed line indicates the maximum yields obtained in this region with direct U-fragmentation. The size of the spots are scaling the cross sections. The limit of identified nuclei on the neutron-rich side correspondsto the present work.

The differential elemental widths of the isotopic distributions σ_N^Z (Fig. 8) are not constant. They increase from 2.1 a.m.u. for light elements up to 3.5 a.m.u. for Pd. The weighted mean value found is (3.3 $\pm$ 0.7) a.m.u., i.e. twice the value found in low-energy fission [14]. The isospin degree of freedom σ_Z^A is softened by a factor of 2.6 compared to thermal neutron fission [13].

To interpret our data more correctly, one has to realize that the observed fission fragments are produced by the fission of many different isotopes. The first stage of the reaction was calculated with the code ABRABLA [24]; The production yields convoluted with the fission probabilities of fragments produced in the reaction Pb(^{238}U,x) were obtained. A mean charge of 87.9 is obtained for the elements feeding the high energy fission process. On Fig.6a is reported the elemental distribution derived from this model when a variance σ of 6 Z-units [25] is assumed for each symmetric partition. The measured distribution is well reproduced except for the lighter elements relatively under-estimated. It points to a larger production of elements lighter than Ra or to lower fission barriers for those elements. The slight decrease in A/Z with Z indicates that more energy is dissipated for the fissions leading to lighter elements. This is compatible with the picture of symmetric fission from a series of parents, the Z and A of which decreases with the violence of the collision. The lightest fragments come from more excited parent nuclei for which the abrasion was deeper.

6 Conclusions

We have shown that by studying ^{238}U fission in inverse kinematics on Pb and Be targets all fragments can be separated by the FRS and identified unambiguously. A large number of isotopes can be studied at the same time and their production yields measured avoiding the uncertainties due to different radio-chemical properties. With the E.M. and L.E. nuclear fission 117 neutron rich isotopes were identified for the first time and their production cross sections were measured. They fill the gap up to the r-process path for elements between Fe and Br and in the region of Sn up to Cs. On the Pb target we have measured systematically the isotopic distributions of fission fragments. The regime of fission consecutive to a phase of abrasion-ablation of the U-projectiles has been retraced from the yields of less neutron-rich nuclei. Fission fragments are clearly identified from U-fragment on the basis of the kinematics. The most probable fragment leading to fission would be a ^{228}Ra excited with 262 MeV, and the fissioning parent a ^{209}Rn at 42 MeV excitation.

References

[1] D. Hilscher and H. Rossner; Annales de physique, Vol.17 (1992) 471

[2] G.Friedlander et al.: Phys.Rev.**129**(1963) 1809

[3] B. D. Wilkins et al. Phys. Rev. Lett. 43 (1979) 1080

[4] B.N. Belyaev, V.D. Domkin, Yu.G. Korobulin; Nucl. Phys. A348 (1980) 479.

[5] M.de Saint Simon et al. Phys. Rev. C26 (1982) 2447

[6] J. Galin et al. Phys. Rev. Lett. 48 (1982) 1787

[7] E. Piasecki et al. Phys. Lett. B377 (1996) 235

[8] S. Polikanov Nucl. Phys. A502 (1989) 195

[9] H. Geissel et al., Nucl. Instr. and Meth. B70 (1992) 286

[10] Bernas M. et al. Phys. Lett. B331 (1994) 19

[11] P. Armbruster et al. Z. Phys. A355 (1996) 191.

[12] Th. Schwab, GSI Report91-10 (1991)

[13] Wahl, A. C.: Atomic and nuclear data tables 39, 1 (1988)

[14] C. Donzaud et al. IPNO 97- to be published in Z. Phys.

[15] Ch. Engelmann et al. Z. Phys. A 352 (1995) 351

[16] M. Hesse et al. Z. Phys. A355 (1996) 69

[17] M. Bernas et al. Nucl. Phys. A616 (1997) 352c

[18] J. Äystö et al., Phys. Rev. Lett. 69 (1992) 1167

[19] K. Sümmerer et al. Phys. Rev. C42 (1990) 2546

[20] J. Benlliure et. al., to be published in Z. Phys. A

[21] V. E. Viola Nucl. Dat. A1 (1966) 391

[22] K.-H. Schmidt et al. Phys. Lett. B300 (1993) 313

[23] J.-J. Gaimard; Ph. D. Thesis, University Paris VII, (1990) and Gaimard J. J. and Schmidt K.-H. Nucl. Phys. A351 (1991) 709

[24] A. Junghans T.H. Darmstadt, Thesis in preparation

[25] S. Steinhaeuser et al. Contribution to the Conference on dynamical aspects of nuclear fission, Casta-Papiernicka, Slovak Republique, Septembre 1996 and Thesis in preparation.